HHS Public Access

Author manuscript

Dev Biol. Author manuscript; available in PMC 2023 December 01.

Published in final edited form as:

Dev Biol. 2022 December ; 492: 1–13. doi:10.1016/j.ydbio.2022.09.005.

The exocyst complex is required for developmental and regenerative neurite growth in vivo

Rachel D. Swope[*],

J. Ian Hertzler[*],

Michelle C. Stone,

Gregory O. Kothe,

Melissa M. Rolls

Biochemistry and Molecular Biology and the Huck Institutes of the Life Sciences, University Park, PA 16802

Abstract

The exocyst complex is an important regulator of intracellular trafficking and tethers secretory vesicles to the plasma membrane. Understanding of its role in neuron outgrowth remains incomplete, and previous studies have come to different conclusions about its importance for axon and dendrite growth, particularly in vivo. To investigate exocyst function in vivo we used Drosophila sensory neurons as a model system. To bypass early developmental requirements in other cell types, we used neuron-specific RNAi to target seven exocyst subunits. Initial neuronal development proceeded normally in these backgrounds, however, we considered this could be due to residual exocyst function. To probe neuronal growth capacity at later times after RNAi initiation, we used laser microsurgery to remove axons or dendrites and prompt regrowth. Exocyst subunit RNAi reduced axon regeneration, although new axons could be specified. In control neurons, a vesicle trafficking marker often concentrated in the new axon, but this pattern was disrupted in Sec6 RNAi neurons. Dendrite regeneration was also severely reduced by exocyst RNAi, even though the trafficking marker did not accumulate in a strongly polarized manner during normal dendrite regeneration. The requirement for the exocyst was not limited to injury contexts as exocyst subunit RNAi eliminated dendrite regrowth after developmental pruning. We conclude that the exocyst is required for injury-induced and developmental neurite outgrowth, but that residual protein function can easily mask this requirement.

Graphical Abstract

Correspondence: mur22@psu.edu.

[*]Equal contributors

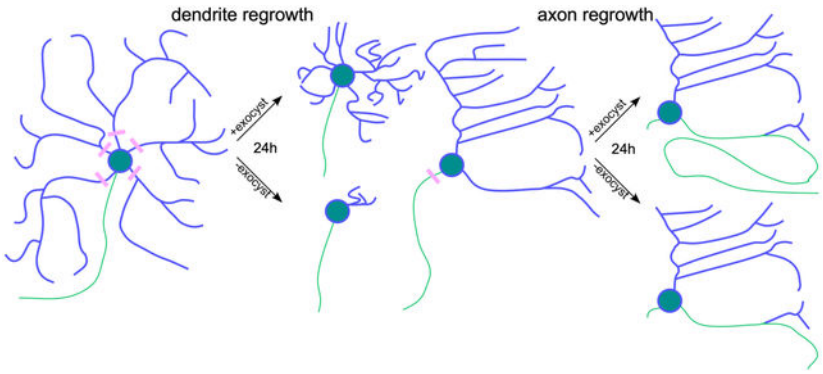

Keywords

Axon; dendrite; regeneration; Sec3; Sec5; Sec6; Sec8; Sec10; Sec15; Exo70; Exo84

Introduction

Axon and dendrite growth involves large scale membrane addition. In most neurons, a single axon grows first and extends over a long distance. This initial extension is then followed by growth of dendrites from multiple tips at once (Craig and Banker, 1994). Classic studies, as well as more recent work using newer approaches, suggest that the strategy for membrane addition is different for axons and dendrites. There are multiple lines of evidence, including accumulation of vesicles in axonal growth cones, suggesting axonal membrane addition occurs at the growth cone (Pfenninger, 2009). Fewer studies have examined dendritic growth or compared axons and dendrites. An early comparative study in hippocampal cultured neurons detected an exogenous membrane protein enriched at the axonal growth cone at early times after expression (Craig et al., 1995). Similar growth cone-enrichment was also seen in minor processes (precursors to dendrites). However, new membrane protein was observed along the length of dendrites once they were specified, rather than in the dendritic growth cone (Craig et al., 1995). More recently, in vivo imaging in Drosophila was used to support the idea that membrane addition occurs along primary dendrites rather than at their tips (Peng et al., 2015). It is therefore possible that different vesicle-targeting machinery underlies these two growth patterns.

SNARE (soluble N-ethylmaleimide-sensitive factor attachment protein receptor) protein pairs on the vesicle and target membrane are sufficient to drive membrane fusion (Weber et al., 1998) and encode some specificity about appropriate vesicle and target matches (McNew et al., 2000). However, fusion events employ protein complexes that act prior to SNARE-driven fusion to dock vesicles (Brown and Pfeffer, 2010; Koike and Jahn, 2022). The exocyst functions as such a docking complex for vesicles destined for plasma membrane incorporation. Originally identified in yeast, the exocyst has been demonstrated to be important for specific fusion events in animal cells, but it is not yet clear whether it is an obligate player in all secretory vesicle-plasma membrane fusion events.

The exocyst is a hetero-octameric complex comprising Sec3, Sec5, Sec6, Sec8, Sec10, Sec15, Exo70, and Exo84. Six of the subunits were identified in a screen for mutants with defects in growth and secretion in budding yeast (Novick et al., 1980), and the remaining two based on association with the complex (Guo et al., 1999; Hsu et al., 1996; Kee et al., 1997; TerBush et al., 1996). The complex is broadly conserved in eukaryotes, including fungi, plants, insects, and mammals (Friedrich et al., 1997; Guo et al., 1997; Hsu et al., 1996; Kee et al., 1997; Murthy et al., 2003; Saeed et al., 2019). Subunits Sec3 and Exo70 recognize phosphatidylinositol(4,5)-bisphosphate (PI(4,5)P_2) at the plasma membrane and Sec15 and Sec4 recognize Rab and SNARE proteins on the secretory vesicle (Heider and Munson, 2012; Polgar and Fogelgren, 2018; Wu and Guo, 2015). Exocyst subunits typically concentrate at sites of vesicle fusion with the plasma membrane (Heider and Munson, 2012; Lepore et al., 2018; Martin-Urdiroz et al., 2016; Wu and Guo, 2015). In budding yeast, temperature-sensitive mutations in exocyst subunits lead to dramatic accumulations of intracellular vesicles (Novick et al., 1980). In multicellular animals, it has been more difficult to determine which exocytosis events require the exocyst. This difficulty stems in part from early lethality of global mutants in mice (Friedrich et al., 1997) and conflicting results about phenotypes, including lethality, in Drosophila (Andrews et al., 2002; Koon et al., 2018; Murthy et al., 2003; Murthy et al., 2005).

In mammalian cell culture, initial studies on epithelial cells suggested that the exocyst was not associated with the plasma membrane before polarization, and was recruited to the plasma membrane efficiently only after cell-cell contact was initiated (Grindstaff et al., 1998), thus implicating exocyst function in polarized, but not general, secretion. In polarized kidney cells, exocyst subunits were specifically localized to lateral membranes and antibody inhibition of Sec8 reduced only basolateral, and not apical, surface delivery (Grindstaff et al., 1998). However, other experiments, including loss of Exo84p in Drosophila embryos have suggested that the exocyst can be involved in apical trafficking in some epithelial cells (Blankenship et al., 2007). Thus, while the exocyst is clearly critical in some types of polarized delivery to the plasma membrane (Martin-Urdiroz et al., 2016; Polgar and Fogelgren, 2018), it remains uncertain how universal its role is.

As in epithelial cells, it is clear that the exocyst plays important roles in at least some types of exocytosis in neurons, but it is unclear how broadly it is involved. Reduction of exocyst subunits in cultured hippocampal or cortical neurons blocks axon specification (Dupraz et al., 2009; Lalli, 2009), perhaps because exocytosis of the IGF-1 receptor fails (Dupraz et al., 2009). This early block in polarization means that the role of the exocyst in axon and dendrite growth could not be assessed in this system. Reduction of exocyst subunits in mouse cortical neurons in vivo also disrupted polarization prior to migration, and so again axon and dendrite growth could not be assessed (Bustos Plonka et al., 2022). Initial studies in Drosophila in which RNAi was used to reduce levels of Sec10, indicated a role for Sec10 only in the secretory ring gland, while nervous system architecture was unaffected (Andrews et al., 2002). This result called into question the importance of the exocyst in neurons in vivo. Subsequent studies examined exocyst function using null alleles of *sec5* or *sec6.* Homozygous mutant animals proceed through embryonic development due to maternal deposits of Sec5 or Sec6, but die as growth-arrested first instar larvae (Murthy et al., 2003; Murthy et al., 2005). Initial nervous system development, including motor axon

outgrowth, occurs in these animals (Murthy et al., 2003; Murthy et al., 2005). However, when neurons were isolated from mutant larvae and challenged to regrow neurites in vitro, initiation of outgrowth failed (Murthy et al., 2003). In vivo, plasma membrane protein addition to axons was strongly reduced in mutant larvae (Murthy et al., 2003; Murthy et al., 2005). Interestingly, synaptic vesicle exocytosis was not disrupted in these backgrounds (Murthy et al., 2003), suggesting some fusion events with the plasma membrane occur without exocyst-mediated docking.

Overall, there are hints that the exocyst is required for axon growth, but definitive evidence that it acts post specification is still quite limited. Moreover, because dendrite growth typically does not proceed without prior axon growth, there is little information about whether the exocyst is important for dendrite extension. In mammalian cultured neurons, partial reduction of an exocyst subunit allowed early neurite outgrowth, but later dendrite branching was reduced (Lira et al., 2019). In vivo, the effect of exocyst loss on dendrites has been examined in Drosophila dendritic arborizaton (da) sensory neurons. These cells innervate the skin with sensory endings that have cell biological signatures of dendrites, including minus-end out microtubules (Rolls et al., 2007; Stone et al., 2008), Golgi outposts (Ye et al., 2007), and ribosomes (Hill et al., 2012). In somatic clones homozygous for null mutations in *Sec5* or *Sec6*, outgrowth of the large dendrite arbor of the dorsal dendritic arborization C (ddaC) neuron was analyzed (Peng et al., 2015). While the major dendrite branches grew out to the edge of their territory, fewer higher order branches were present, and the total arbor length was shorter than in control neurons (Peng et al., 2015). Thus, the data so far suggests that the exocyst is required for higher order dendrite growth, but perhaps not initial outgrowth. Moreover, it remains ambiguous whether the axon is more dependent on the exocyst for outgrowth than dendrites.

While these studies suggest that the exocyst is critical for neuronal polarization, and likely also axon growth and higher order dendrite branching, analysis of *exo70* phenotypes in Drosophila yield a much more nuanced picture. Surprisingly, animals homozygous for mutant *exo70* without detectable exo70 transcript are viable and have broadly normal nervous system architecture (Koon et al., 2018). Instead, specific defects at the neuromuscular junction and sensitivity to heat stress were described (Koon et al., 2018), suggesting that Exo70 is not absolutely required for neuron growth under normal conditions.

Here we aim to broadly test whether the exocyst is required for axon and dendrite outgrowth in vivo. We bypass requirements for exocyst function in early development by using neuron-specific RNAi to reduce exocyst subunits in Drosophila da neurons. As in previous studies using mutant clone approaches in Drosophila, initial outgrowth of axons and dendrites was able to occur in exocyst-reduced neurons. We therefore challenged neurons to regrow axons and dendrites after laser-mediated removal. RNAi of all seven subunits tested dramatically reduced dendrite regeneration, and axon regeneration was also severely impaired, although a new axon could still be specified. To test whether this represented a specific strong requirement for the exocyst in injury-induced regeneration, we tested developmental dendrite regrowth after pruning. This type of neurite growth was also blocked. We conclude that axon and dendrite outgrowth in vivo is strongly dependent on the exocyst.

Results

Initial axons and dendrite outgrowth occurs in neurons with exocyst subunits targeted by RNAi

To test exocyst function in neurons in vivo, we used a cell-type specific RNAi approach. The binary Gal4-UAS expression system was used to drive expression of RNA hairpins as well as cell shape markers in neuron subsets using specific Gal4 drivers and UAS-driven transgenes (Brand and Perrimon, 1993; Dietzl et al., 2007). UAS-Dicer-2 was included to enhance RNAi efficacy in neurons (Dietzl et al., 2007). We first assayed development of normal morphology of simple and complex dendrite arbors of larval Drosophila da neurons. The ddaE neuron is a representative of the simplest class of da neurons (Grueber et al., 2002) and responds to folding of the cuticle during larval locomotion (He et al., 2019; Vaadia et al., 2019). The ddaC neuron belongs to the most complex class of da neurons (Grueber et al., 2002) and responds to nociceptive stimuli including ovipositor insertion of parasitoid wasps (Hwang et al., 2007). In 3-day old larvae, dendrite arbors of both neuron types with exocyst components knocked down appeared identical in complexity to control. While class 1 ddaE neurons had the same number of dendrite branches as control (Figure 1A-B), they did appear slightly beaded. Class 4 ddaC neurons appeared identical to control (Figure 1C). To quantify this complexity, we traced the entire dendrite arbor of 5-10 neurons per genotype and performed a Sholl analysis with 10 μm steps. No significant differences were seen in complexity (Figure 1E) or total dendrite length (Figure 1F) between any genotypes. We also examined axonal projections of class 4 neurons to the ventral nerve cord, and observed that axons reached their target in control and Sec6 RNAi neurons (Figure 1D). Thus, initial axon and dendrite outgrowth occurred in neurons with exocyst subunits reduced by RNAi. Previous analysis of ddaC neuron *Sec5* and *Sec6* mutant clones demonstrated reduced dendrite branching (Peng et al., 2015), so the acquisition of normal neuronal morphology was likely due to residual exocyst function in our RNAi neurons.

The exocyst complex is required for sensory axon regeneration in vivo

We hypothesized that small amounts of exocyst complex may support initial neurite outgrowth, but that neurons may not be able to respond to the challenge of regrowing an axon after its removal. By definition, cell-type specific RNAi is induced after a particular cell is born, so it typically becomes more effective over time. The delay between initial axonal development and our assay for regrowth was two to three days. When the axon of larval ddaE neurons is severed proximally (10-20 μm from the soma), the neuron specifies a dendrite to become a new axon by flipping its microtubule polarity and initiating outgrowth from the dendrite tip (Rao and Rolls, 2017; Stone et al., 2010). By 96 hours post axotomy (HPA), the chosen dendrite has, on average, grown several hundred microns in the body wall as it wanders in search of a target to grow along. If it encounters the nerve, it grows along it towards the central nervous system (Rao and Rolls, 2017). We performed proximal axotomy on two-day old Drosophila larvae. While neurons expressing a control RNAi hairpin grew a new axon averaging over 200μm by 96HPA (Figure 2A and 2D), neurons with RNAi knockdown of exocyst complex members Sec5, Sec6, Sec8, Sec10, and Sec15 had reduced regeneration (Figure 2B-D). RNAi experiments were performed using tester lines that contained UAS-Dicer-2 (see Reagent Table). Dicer-2 is included to improve efficacy of

long hairpin RNAs in neurons (Dietzl et al., 2007). We used a mixture of RNAi lines from collections at the Bloomington Drosophila Stock Center (BDSC) and the Vienna Drosophila Resource Center (VDRC) (see Reagent Table for details) and whether a phenotype was seen did not depend on the source (control, Sec5A and Sec6 RNAi lines were from VDRC, and Sec8, Sec10, Sec15 and Exo70 were TRiP lines from BDSC). The reduction of axon regeneration by targeting many different exocyst subunits strongly suggests that the exocyst complex is required for this form of polarized neuronal outgrowth.

Failure of axon outgrowth in cultured rodent neurons has been suggested to be downstream of lack of insertion of the IGF-1 receptor in the plasma membrane and axon specification (Dupraz et al., 2009). To determine whether the new axon was correctly specified after proximal axotomy, we analyzed microtubule polarity. In uninjured da neurons, dendrites have almost exclusively minus-end-out microtubule polarity, while axons have plus-end-out polarity (Rolls et al., 2007; Stone et al., 2008). When a dendrite is converted to a regenerating axon, the microtubules are rebuilt to plus-end-out before growth is initiated (Stone et al., 2010), and if this does not occur outgrowth does not happen (Mattie et al., 2010). Microtubule plus end-binding proteins including EB1 can be used to track the polarity of microtubules in living neurons (Rolls et al., 2007; Stepanova et al., 2003), so we expressed EB1-GFP in ddaE neurons with control or Sec6 RNAi transgenes. Microtubule polarity in uninjured Sec6 RNAi neurons was almost identical to control, with predominantly minus-end-out dendrites, and no dendrites that had majority plus-end-out microtubules (Figure 3B). Sec6 RNAi was chosen for additional analysis as it resulted in a strong axon regeneration defect (Figure 2D). All major dendrite branches (red dotted lines, Figure 3A) were analyzed for microtubule polarity at 96h after axotomy. All control neurons converted a dendrite to plus-end-out polarity (Figure 3B and C). The same conversion was seen in all Sec6 RNAi neurons (Figure 3B and C), indicating that a new axon could be specified. This result suggests that regeneration failure in Sec6 RNAi neurons occurs downstream of axon specification.

Accumulation of a membrane trafficking marker in the regenerating axon depends on the exocyst

Axons are thought to grow by membrane addition near the growing tip (Pfenninger, 2009). Synaptotagmin-GFP (syt-GFP) has been used as a marker for post-Golgi traffic in multiple cell types in Drosophila (Murthy et al., 2003; Yamanaka et al., 2015). Moreover, endogenous synaptotagmin has been used as a vesicle marker in differentiating PC12 cells, and concentrates in growth cones with Exo70 (Vega and Hsu, 2001). We hypothesized that syt-GFP would concentrate in in regenerating axon tips similarly to PC12 growth cones. In addition, we anticipated that syt-GFP vesicles should also concentrate in new axons in neurons with reduced exocyst function as these cells specify a neurite with axonal microtubule polarity (Figure 3). If microtubules direct secretory traffic to the correct place, and the exocyst functions at the fusion step, then syt-GFP could also concentrate at higher levels in regenerating axons of exocyst RNAi neurons. To test these predictions, we generated a tester line with UAS-Dicer-2, UAS-mCD8-mCherry, and UAS-syt-GFP driven in class I ddaE neurons with 221-Gal4. In uninjured neurons, syt-GFP was ubiquitous throughout the axon, soma, and dendrites, localizing in a punctate pattern, with bright

spots of Golgi visible in the cell body (Figure 4A). A similar distribution was observed in uninjured Sec6 RNAi neurons (Figure 4B). To see whether syt-GFP redistributed during axon regeneration, we severed axons of class I ddaE neurons and imaged them 72 hours later during active axon outgrowth. Neurons were categorized based on whether they exhibited regenerative outgrowth, and on the pattern of syt-GFP distribution. Example images of the different patterns are included in Figure 4 and Figure S1. In control neurons that regenerated, syt-GFP was often concentrated in the regrowing axon, although about half of the cells also had some fluorescence elsewhere (Figure 4A and 4C). Neurons that had syt-GFP concentrated only in the new axon (tip and tip + shaft category) no longer had detectable syt-GFP in the cell body. In similar experiments using a previously generated UAS-GFP-Sec15 (Jafar-Nejad et al., 2005; Peng et al., 2015), the GFP signal was too dim to be reliably detected during regeneration. Rather than having syt-GFP more strongly concentrated in a single neurite, injured Sec6 RNAi neurons had a more variable syt-GFP than control neurons. Moreover, many non-regenerating neurons did not concentrate syt-GFP to a particular neurite (Figure 4B and C), even though cells were able to specify new axons based on microtubule polarity (Figure 3). Our data suggests that targeting of post-Golgi vesicles to newly specified axons is influenced by the exocyst complex, suggesting that it acts downstream of microtubule polarity, but perhaps at a step upstream of membrane fusion.

The exocyst complex is required for dendrite regeneration in vivo

Dendrite growth is thought to be mediated by distributed membrane addition along dendrite trunks, rather than targeted exocytosis at the tip (Peng et al., 2015). We therefore considered that dendrite regrowth may not be as dependent on the exocyst as axon regeneration. We used a post-developmental regeneration assay similar to the approach used above for the axon to test the requirement of exocyst subunits in dendrite growth. Dendrite regeneration in class 4 ddaC neurons involves much more outgrowth than dendrite regeneration of ddaE (Stone et al., 2014; Thompson-Peer et al., 2016), and is easier to assay. When all dendrites are severed near the cell body, ddaC neurons regenerate a robust arbor that returns to cover its original receptive field by 96 hours after injury (Stone et al., 2014). Unlike axon regeneration, which is often not initiated until 24 or 48h after injury (Stone et al., 2010; Stone et al., 2012), dendrite regeneration begins around 6-8h post injury, and by 24h the new arbor is large enough to use as a metric for dendrite regeneration candidate screening (Nye et al., 2020). We cut all dendrites off of ddaC neurons expressing control or exocyst subunit RNAi transgenes and assayed the new arbor 24h later. Control neurons generated a new arbor spanning almost 300 microns (Figure 5A, left and 5B) and comprising over 3000 microns of new growth (Figure 5C). This amount of outgrowth is an order of magnitude higher than that seen after axon injury at 96h. New arbors also gained on average over 100 branch points in the first 24h (Figure 1D). Regeneration of exocyst RNAi neurons was severely attenuated (Figure 5A, right) in terms of arbor diameter as well as total new dendrite length and number of branch points (Figure 5B-D). Interestingly, genotypes that had mild or no axon regeneration deficit still had a strong reduction in dendrite regeneration, perhaps due to the much higher demand for membrane in a shorter time frame.

Since syt-GFP concentrated in regenerating axons, we wondered if it would redistribute in regenerating dendrites. To assess this, we crossed flies expressing 477-Gal4 and mCD8-mCherry to flies with syt-GFP. Before injury, synaptotagmin was clearly visible in the cell body, and present in spots in dendrites, particularly those close to the cell body (Figure 6A). 18 hours after dendrite injury, the new dendrite branches had been populated with syt-GFP puncta in much the same manner as uninjured cells (Figure 6B). Distal tips of regenerating dendrites were quite dim; however, a few puncta were seen in tips and many puncta were visible throughout the new dendrite. Similar dispersed puncta were observed in 7 neurons imaged 18h after injury and 6 neurons imaged 24h after injury. Thus, although the exocyst was strongly required for dendrite regrowth, we did not find evidence that membrane delivery was regionally targeted.

Dendrite regrowth after pruning requires the exocyst complex

Dendrite regeneration has been suggested to be different from developmental dendrite outgrowth (Thompson-Peer et al., 2016), so we wished to determine whether the exocyst was also required for dendrite growth that was not initiated in response to injury. Dendrites of many da neurons including Class 4 are pruned during early pupal development, and then new dendrite arbors grow into the adult body wall (Shimono et al., 2009). Dendrites of the ventral class 4 neuron, v'ada, can be visualized in the adult abdomen (Shimono et al., 2009). To test whether developmental regrowth of v'ada required the exocyst complex, we knocked down Sec6 and Sec15 and examined v'ada neurons in adult flies. Control neurons regrew a large arbor that is slightly morphologically different from its larval form but still covers a large receptive field (Figure 7A). When Sec6 or Sec15 was knocked down, there was almost no regrowth of dendrites (Figure 7B and C). The cells had beaded axons and appeared to be in the process of dying. This phenotype was consistent across 5-6 adult flies imaged per genotype. Thus, the requirement for the exocyst in neurite outgrowth is not restricted to growth induced by injury.

Discussion

It has historically been difficult to definitively answer the question of whether the exocyst complex is essential for the polarized extension of axons and dendrites. In primary neuron cultures, axon specification is blocked when exocyst subunits are reduced and so neuronal development is arrested before axons and dendrites initiate large scale growth (Dupraz et al., 2009). In mice, mutant embryos die too early to assay neuronal morphology (Friedrich et al., 1997). In Drosophila, maternal deposits of Sec5 and Sec6 persist for several days after egg laying and support initial nervous system development (Murthy et al., 2003; Murthy et al., 2005), then animals die. In contrast, *exo70* mutant animals are homozygous viable (Koon et al., 2018). We bypassed some of these issues by using cell-type specific RNAi to knock down 7 exocyst subunits in Drosophila model sensory neurons. This approach allowed initial neuronal development to occur, likely because of remaining exocyst function. This initial development meant that comparison of axon and dendrite outgrowth was not hampered by early failure of axon outgrowth precluding analysis of subsequent dendrite growth. We could test axon and dendrite regrowth independently by complete removal of the axon or the dendrite arbor. Regrowth was initiated two to three days after initial neuronal development,

which allowed run-down of remaining protein. Physical removal of the axon or dendrite should also have further depleted exocyst levels because any complex that was in the severed region would no longer be available for reuse. We found that axon and dendrite regeneration were severely impaired in neurons with reduced exocyst subunits. For axon regeneration, the block occurred after a new axon was specified. By examining dendrite regrowth after pruning, we were able to show that the requirement for neurite outgrowth was not specific to injury-induced extension.

One unresolved question about neurite outgrowth is whether axons and dendrites use the same molecular mechanisms to add new membrane lipids and proteins to their plasma membrane during large, polarized outgrowth events. Axons and dendrites have distinct morphologies and their construction entails different subcellular events. For example, the smooth endoplasmic reticulum (ER) becomes enriched at the tip of regenerating axons, but not dendrites, in Drosophila (Rao et al., 2016) and outgrowth of mammalian axons in culture is associated with enrichment of ER tubules in the distal axon (Farias et al., 2019) and ER concentration in the growth cone (Deitch and Banker, 1993; Pavez et al., 2019; Petrova et al., 2020). In addition, Golgi outposts are found in dendrites and not axons (Horton et al., 2005) and dendrite growth seems more sensitive to disruption of Golgi-mediated secretion than axons (Horton et al., 2005; Ye et al., 2011). However, here we show that both axon and dendrite regeneration rely on the exocyst complex, which tethers Golgi-derived vesicles to the PM for fusion, suggesting that vesicle-based transport of new membrane materials from the Golgi is critical for both types of growth.

While our results do not support the idea that axons and dendrites are differentially dependent on exocyst-mediated secretion, they are consistent with previous studies that indicate the two types of neurites add membrane with different spatial strategies. Growing axons are generally thought to add membrane at their tip (Pfenninger, 2009; Vance et al., 2000), while dendrites seem to add membrane more broadly, including along their main trunk (Peng et al., 2015). While not definitive, the difference in distribution of the membrane trafficking marker syt-GFP during axon and dendrite regeneration is consistent with membrane delivery to concentrated regions of the axon and more dispersed delivery to dendrites. One potential reason for this difference is microtubule polarity. Early in dendrite regeneration, microtubule polarity is mixed (Feng et al., 2019; Stone et al., 2014), while axons regenerating from dendrites have plus-end-out polarity (Stone et al., 2010). In mammalian dendrites mixed microtubule polarity has been suggested to lead to distributed cargo delivery (Kapitein et al., 2010). However, there are two flaws in the simple model that uniform microtubule polarity leads to localized membrane delivery. First, in mature Drosophila neurons, dendrite polarity becomes uniform (minus-end-out) (Hill et al., 2012), but membrane addition is still distributed along the main dendrite (Peng et al., 2015). Second, we found that all Sec6 RNAi neurons converted a dendrite to plus-end-out polarity (Figure 3), but only a subset accumulated syt-GFP in concentrated regions of the cell (Figure 4) suggesting that plus-end-out polarity is not sufficient to drive membrane cargos to specific regions of the new axon when the exocyst is reduced. This second result hints that the exocyst could play a role in vesicle targeting as well as fusion in neurons.

One source of confusion on studies of exocyst function in vivo has been that different results have been obtained in studies focused on specific subunits. Therefore, it has been ambiguous whether all subunits are equally important. For example, analysis of *exo70* mutants in Drosophila led to the conclusion that this subunit is only required for neurite extension under heat stress conditions (Koon et al., 2018), while Sec10 RNAi neurons had no detectable phenotypes (Andrews et al., 2002), and Sec5 and Sec6 mutant clones exhibited simplified dendrite arbors (Peng et al., 2015). The *exo70* mutants used were transposon insertion alleles, rather gene deletions, and so it is possible small amounts of protein were produced (Koon et al., 2018). Similarly, while global levels of Sec10 were reduced in the early RNAi study (Andrews et al., 2002), this was prior to inclusion of Dicer-2 expression to facilitate neuronal knockdown and so, again, some protein may have remained in neurons. We find that knockdown of each of the 7 subunits we tested led to the same strong reduction of dendrite regeneration. In contrast, no defects in initial outgrowth were observed. The simplest explanation for all of the data taken together, from our work and previous studies, is that all exocyst subunits are equally important for neurite outgrowth, but that even very small amounts of residual protein can provide enough function to mask this requirement.

Materials and methods

Drosophila stocks

RNAi lines used here were obtained from the Bloomington Drosophila Stock Center (NIH P40OD018537) and the Vienna Drosophila Resource Center (Table 1). Transgenic tester lines used include: (UAS-Dicer-2; 221:Gal4, UAS-mCD8-GFP), (UAS-Dicer-2; 221:Gal4, UAS-EB1-GFP), (477-Gal4, UAS-mCD8-RFP), (ppk:Gal4, ppk:EGFP, ppk:CD4-tdGFP, nls-BFP-UAS-Dicer-2); UAS-mCD8-mCherry, UAS-Dicer-2; 221-Gal4, UAS-syt-GFP) (Table 1). Larvae for experiments were selected from the offspring of crosses between female virgins of the tester lines and males of RNAi lines. Crosses were set up in a bottle with a food cap at the bottom. Caps were collected and replaced every 24 hours and stored at 25°C for either 2 days (axon regeneration experiments) or 3 days (all other experiments) before use. Ingredients for 10L of fly food media: 45g Agar, 259g Sucrose, 517g Dextrose, 155g yeast, 858g cornmeal, 40 mL 10% tegosept in ethanol, 60mL proprionic acid.

Generation of transgenic UAS-Dicer-2 linked to a visible marker

Overview: To facilitate assembly of recombinant Drosophila chromosomes with multiple transgenes, we wished to generate a UAS-Dicer-2 (Dcr-2) transgene that could be tracked by fluorescent microscopy. The UAS-Dcr-2 transgene we have previously used to enhance neuronal RNAi (Dietzl et al., 2007) requires PCR to detect. The basic idea was to use an eye-specific promoter (PXP3) to drive BFP in the same P element insertion vector as the UAS-Dcr-2. The P element would include the standard miniwhite element, and PXP3-3XTagBFP2 followed by UAS-Dcr-2. We made versions that included soluble 3XTagBFP2 and versions in which it was targeted to the nucleus with a nuclear localization sequence (nls). While our original intent was that the 3XTagBFP2 would be detectable only in the eye, the placement of the sequence immediately upstream from the UAS element allows it to be driven in the same pattern as the Dcr-2; the UAS acts as a Janus promoter

in this construct and Gal4-binding to it results in expression of upstream and downstream coding sequences.

Plasmid construction: The following primers were used to PCR amplify the complete Dcr-2 ORF from Drosophila cDNA clone FI15132 (DGRC Stock 1644347) using Herculase DNA polymerase (Agilent 600675):

Dcr2F1

ATTGGGAATTCGTTAACAGATCTAAGATATGGAAGATGTGGAAATCAAGCCTCG

Dcr2R1

GTTCCTTCACAAAGATCCTCTAGATTAGGCGTCGCATTTGCTTAGCTGCTGAAGGGC

The gel purified product was cloned into BglII-XbaI digested pUAST by In-Fusion (TaKaRa 638948) to produce pUAST-Dcr-2. A plasmid on hand in the lab that had previously been generated for Drosophila CRISPR, termed 1GCT_pHD-dsRed, was used to clone 3XTagBFP2 downstream of the Drosophila 3XP3 promoter. The following primers were used to PCR amplify 3XTagBFP2 from pHAGE-TO-nls-st1dCas9-3nls-3XTagBFP2 (Addgene 64512):

BFP2F1 (to include nls)

ACCATGGCCTCCTCCGAGGACGTCGGCTCTACTAGTGGCCCCAAGAAGAAGAGG

BFP2F2 (to exclude nls)

ACCATGGCCTCCTCCGAGGACGTCGGATCCGGAAGTATGGTGTCTAAGGGCG

BFP2R1

GCGCGCTCGTACTGCTCCACGATGGTGCTACTCGAGATTAAGCTTGTGCCCCAG

The PCR products were cloned into AatII-AleI digested 1GCT_pHD-dsRed by In-Fusion to generate constructs 1GCT_BFP2_F1 and 1GCT_BFP2_F2, with and without nuclear localization signals, respectively. The following primers were used to PCR amplify 3XP3-(nls)-3XTagBFP2 using the 1GCT_BFP constructs as template:

3XP3BFP2F1

CGGAGGACAGTACTCCGACCTGCAGGCGTACGGGATCTAATTCAATTAGAG

3XP3BFP2R1

CGGATCCAAGCTTGCATGACCGGTTAAGATACATTGATGAGTTTGG

The PCR products were cloned by In-Fusion into SbfI digested pUAST-Dcr-2 to generate the final products (pUAST-3XP3-3XTagBFP2-UAS-Dcr-2 and pUAST-3XP3-nls3XTagBFP2-UAS-Dcr-2). Complete plasmid sequences have been deposited to GenBank.

Plasmids were injected into Drosophila embryos by BestGene (https://www.thebestgene.com/), and resulting transgenic flies were mapped to chromosomes and used to generate recombinant tester lines as indicated (Table 1).

Larval mounting for imaging and neuron selection

For all experiments, larvae were mounted dorsal side up to a glass slide on top of a thin dried agar pad with a coverslip taped on top. Larvae were immobilized by pressure of the coverslip; no anesthetics were used. There are 8 abdominal body segments in larva, and each contain a dorsal and ventral cluster of neurons, including the class I ddaE and class IV ddaC. For all experiments, one neuron was used per animal within the second to fourth abdominal segments.

Image acquisition and analysis

Zeiss microscopes (Thornwood, NY) were used to acquire all images for this study. We used the following systems:

LSM800 inverted confocal on an Axio Observer Z1 stand and equipped with GaAsP detectors and a Zeiss Plan-APOCHROMAT 63x DIC (oil, 1.4NA) objective;

LSM800 upright confocal on an Axio Imager.Z2 stand and equipped with GaAsP detectors and Zeiss Plan-APOCHROMAT 63x DIC (oil, 1.4NA) and Zeiss Plan-APOCHROMAT DIC (UV) VIS-IR 40x (oil, 1.3NA) objectives;

Zeiss Axio Imager.M2 widefield equipped with an AxioCam 506 mono camera and Zeiss Plan-APOCHROMAT 63x DIC (oil, 1.4NA), Zeiss EC Plan NEO FLUAR 40x (oil, 1.3NA) objectives.

All images for localization experiments were taken with a 63x 1.4 NA oil objective; all 0-hour images for injury experiments were taken with a 63x 1.4 NA oil objective; and all 24-hour, 72-hour, and 96-hour post injury images were taken with a 40x 1.3 NA oil objective. Adult v'ada neuron images were taken on 10x and 20x air objectives. All images were processed in FIJI software (https://imagej.net/software/fiji/). Z-stacks and time series images were converted to maximum-intensity projections with the z-project function. Occasionally, clean maximum intensity projections were rendered impossible due to larval movement during imaging; when this was the case, we used the stitching plugin (max intensity option) to generate a complete image.

Class I and IV morphology analysis

Images of full class I and IV neuron arbors in 3-day old larva were obtained with a Zeiss LSM800 confocal microscope. The z-stacks were maximum projected so that all dendrites of the neuron were in a 1-frame, 2-dimensional image (no depth). For class I neurons, number of total dendrite branch points per neuron was counted. For class IV, dendrites were

traced with the simple neurite tracer (SNT) plugin on FIJI (https://imagej.net/software/fiji/) and a Sholl analysis was performed within the SNT plugin (Schindelin et al., 2012). The concentric circles were placed in 10 μm steps from the center of the cell body. 5-9 neurons were quantified per genotype. For the dendrite regeneration morphology quantified in Figure 5, the same FIJI plugin and analysis was used as for uninjured neurons.

Class I axon regeneration assay

These experiments were performed per the protocol described in (Hertzler et al 2020). Briefly, the axon of a class I neuron was severed 10-20μm from the soma using a MicroPoint UV pulsed laser. An image was taken on a Zeiss widefield microscope, and the larva was returned to a food cap at 20°C for 96 hours. An image was then taken of the same neuron 96 hours post injury. Normalized axon regeneration was quantified as:

$$\text{Regeneration} = (\text{Length}_{\text{96hr new axon}} - (\text{Length}_{\text{0hr new axon}} * (\text{Length}_{\text{96hr control dendrite}} / \text{Length}_{\text{0hr control dendrite}})))$$

Class I microtubule polarity

Videos of individual neurons were taken on a Zeiss Axio Imager.M2 widefield microscope at 1 frame per second for 5 minutes (300 frames). Since not all the dendrites lie in exactly the same z plane, roughly half of the 5-minute video was spent focused on the comb dendrite (Figure 3A, top dotted line) and the other half was spent on the secondary dendrites (Figure 3A, right and bottom dotted lines) to get an idea of polarity in all main dendrites and avoid excessive photobleaching of the EB1-GFP. A dendrite was classified as plus-end out if 75% or more of the visible microtubules polymerized away from the cell body. Kymographs were generated from videos of both genotypes at 96 hours post injury and uninjured cells by drawing a segmented line over a section of in-focus dendrite and using the multi-kymograph plugin (line width 3) in FIJI. When the line is drawn towards the cell body, minus-end out comets travel to the right and plus-end out comets travel to the left in kymographs.

syt-GFP imaging

For class I axon injury, syt-GFP and the mCD8-mCherry cell shape marker were overexpressed with Gal4 under the 221 promoter. Axon severing and imaging were performed on an LSM800 microscope equipped with MicroPoint UV laser. An image was taken of neurons in 2-day old larva before the axon was severed 10-20μm from the cell body. After axon injury, the larvae were returned to a food cap for 3 days at 25°C or 4 days at 20°C, which are approximately equivalent. Data from both 72hr and 96hr experiments were pooled for quantification as there is no discernable difference between those time points. During these experiments images were acquired with different microscope settings, but in all conditions syt-GFP was visible and all images are included in quantification.

For class IV dendrite injury, syt-GFP and mCD8-mCherry were driven by 477-Gal4. Dendrites were severed using a MicroPoint UV pulsed laser on an LSM800 inverted confocal microscope and larvae were returned to a food cap for 24 hours at 25°C. Images were acquired 24h after injury on the same microscope.

Since syt-GFP distribution was not uniform after axon injury, we set 8 total categories for quantifying, 3 for those with no regeneration and 5 for those with regeneration. “None” indicates no visible syt-GFP; “Localized” indicates that syt was grouped in 1 or more specific dendrites, notably different from “dispersed,” which had puncta throughout the dendrite arbor. No neurons that regenerated a new axon had no syt signal; all regenerating neurons across both control and Sec6 RNAi genotypes had syt-GFP at least in the growing tip (>10μm of green signal), tip+shaft, where most of the new axon contained syt puncta; tip+shaft+elsewhere, where the new axon and its tip contained syt puncta but other non-growing dendrites did as well, or dispersed, where syt was present in the new axon tip as well as everywhere else in the arbor. All pre-injury images of both control and Sec6 RNAi neurons had dispersed syt-GFP. Examples of the categories are shown in Figure 4 and Figure S1.

Class IV dendrite regeneration assay

These experiments were performed per the protocol described in (Hertzler et al 2020). Briefly, the dendrites of one class IV neuron in a 3-day old larva were severed using a MicroPoint UV pulsed laser on a Zeiss Axio Imager.M2 widefield microscope. The larva was recovered and placed in a food cap at 25°C for 24 hours and then imaged on a Zeiss LSM800 confocal microscope. For quantification, a line was drawn across the new dendrites at the widest possible point, this being the regeneration diameter. Neurons were also traced with the SNT plugin on FIJI and a Sholl analysis was performed on injured neurons the same way as uninjured neurons in Figure 1.

Class IV adult neuron imaging

Crosses were set up using the same transgenic lines as the dendrite regeneration assay, as the ppk promoter still labels these Class 4 neurons after pupariation. Larvae were collected and allowed to pupate and eclose. Newly eclosed adults (less than 8 hours) were used for imaging as their abdomen is usually much less opaque than older adults. Adults were knocked out with CO_2, had their wings and lower set of legs snipped off, and mounted under a coverslip with a thin coating of glycerol to allow optical contact between the abdomen and glass. Tiled z-stacks were taken of the abdomen region with a Zeiss LSM800 inverted confocal microscope.

Statistical analysis

GraphPad Prism software was used to generate graphs and perform statistical analysis. Figure legends contain information about statistical tests used. Significance is shown as * ($p<.05$), ** ($p<.01$), *** (p.001), and all error bars represent standard deviation.

Supplementary Material

Refer to Web version on PubMed Central for supplementary material.

Acknowledgements

We are very grateful to the Bloomington Drosophila Stock Center (NIH P40OD018537) and the Vienna Drosophila Resource Center for providing transgenic lines used in this study. We are also grateful to Dr. Mary Munson for

discussions that helped initiate this project, and members of the Rolls lab for input along the way. Funding for the project was provided in part by the National Institutes of Health, GM085115.

References

Andrews HK, Zhang YQ, Trotta N, and Broadie K. 2002. Drosophila sec10 is required for hormone secretion but not general exocytosis or neurotransmission. Traffic. 3:906–921. [PubMed: 12453153]

Blankenship JT, Fuller MT, and Zallen JA. 2007. The Drosophila homolog of the Exo84 exocyst subunit promotes apical epithelial identity. Journal of cell science. 120:3099–3110. [PubMed: 17698923]

Brand AH, and Perrimon N. 1993. Targeted gene expression as a means of altering cell fates and generating dominant phenotypes. Development. 118:401–415. [PubMed: 8223268]

Brown FC, and Pfeffer SR. 2010. An update on transport vesicle tethering. Mol Membr Biol. 27:457–461. [PubMed: 21067454]

Bustos Plonka F, Sosa LJ, and Quiroga S. 2022. Sec3 exocyst component knockdown inhibits axonal formation and cortical neuronal migration during brain cortex development. J Neurochem. 160:203–217. [PubMed: 34862972]

Craig AM, and Banker G. 1994. Neuronal polarity. Annual review of neuroscience. 17:267–310.

Craig AM, Wyborski RJ, and Banker G. 1995. Preferential addition of newly synthesized membrane protein at axonal growth cones. Nature. 375:592–594. [PubMed: 7791876]

Deitch JS, and Banker GA. 1993. An electron microscopic analysis of hippocampal neurons developing in culture: early stages in the emergence of polarity. The Journal of neuroscience : the official journal of the Society for Neuroscience. 13:4301–4315. [PubMed: 8410189]

Dietzl G, Chen D, Schnorrer F, Su KC, Barinova Y, Fellner M, Gasser B, Kinsey K, Oppel S, Scheiblauer S, Couto A, Marra V, Keleman K, and Dickson BJ. 2007. A genome-wide transgenic RNAi library for conditional gene inactivation in Drosophila. Nature. 448:151–156. [PubMed: 17625558]

Dupraz S, Grassi D, Bernis ME, Sosa L, Bisbal M, Gastaldi L, Jausoro I, Caceres A, Pfenninger KH, and Quiroga S. 2009. The TC10-Exo70 complex is essential for membrane expansion and axonal specification in developing neurons. The Journal of neuroscience : the official journal of the Society for Neuroscience. 29:13292–13301. [PubMed: 19846717]

Farias GG, Freal A, Tortosa E, Stucchi R, Pan X, Portegies S, Will L, Altelaar M, and Hoogenraad CC. 2019. Feedback-Driven Mechanisms between Microtubules and the Endoplasmic Reticulum Instruct Neuronal Polarity. Neuron.

Feng C, Thyagarajan P, Shorey M, Seebold DY, Weiner AT, Albertson RM, Rao KS, Sagasti A, Goetschius DJ, and Rolls MM. 2019. Patronin-mediated minus end growth is required for dendritic microtubule polarity. The Journal of cell biology. 218:2309–2328. [PubMed: 31076454]

Friedrich GA, Hildebrand JD, and Soriano P. 1997. The secretory protein Sec8 is required for paraxial mesoderm formation in the mouse. Developmental biology. 192:364–374. [PubMed: 9441674]

Grindstaff KK, Yeaman C, Anandasabapathy N, Hsu SC, Rodriguez-Boulan E, Scheller RH, and Nelson WJ. 1998. Sec6/8 complex is recruited to cell-cell contacts and specifies transport vesicle delivery to the basal-lateral membrane in epithelial cells. Cell. 93:731–740. [PubMed: 9630218]

Grueber WB, Jan LY, and Jan YN. 2002. Tiling of the Drosophila epidermis by multidendritic sensory neurons. Development. 129:2867–2878. [PubMed: 12050135]

Guo W, Grant A, and Novick P. 1999. Exo84p is an exocyst protein essential for secretion. The Journal of biological chemistry. 274:23558–23564. [PubMed: 10438536]

Guo W, Roth D, Gatti E, De Camilli P, and Novick P. 1997. Identification and characterization of homologues of the Exocyst component Sec10p. FEBS Lett. 404:135–139. [PubMed: 9119050]

He L, Gulyanon S, Mihovilovic Skanata M, Karagyozov D, Heckscher ES, Krieg M, Tsechpenakis G, Gershow M, and Tracey WD Jr. 2019. Direction Selectivity in Drosophila Proprioceptors Requires the Mechanosensory Channel Tmc. Current biology : CB. 29:945–956 e943. [PubMed: 30853433]

Heider MR, and Munson M. 2012. Exorcising the exocyst complex. Traffic. 13:898–907. [PubMed: 22420621]

Hill SE, Parmar M, Gheres KW, Guignet MA, Huang Y, Jackson FR, and Rolls MM. 2012. Development of dendrite polarity in Drosophila neurons. Neural Dev. 7:34. [PubMed: 23111238]

Horton AC, Racz B, Monson EE, Lin AL, Weinberg RJ, and Ehlers MD. 2005. Polarized secretory trafficking directs cargo for asymmetric dendrite growth and morphogenesis. Neuron. 48:757–771. [PubMed: 16337914]

Hsu SC, Ting AE, Hazuka CD, Davanger S, Kenny JW, Kee Y, and Scheller RH. 1996. The mammalian brain rsec6/8 complex. Neuron. 17:1209–1219. [PubMed: 8982167]

Hwang RY, Zhong L, Xu Y, Johnson T, Zhang F, Deisseroth K, and Tracey WD. 2007. Nociceptive neurons protect Drosophila larvae from parasitoid wasps. Current biology : CB. 17:2105–2116. [PubMed: 18060782]

Jafar-Nejad H, Andrews HK, Acar M, Bayat V, Wirtz-Peitz F, Mehta SQ, Knoblich JA, and Bellen HJ. 2005. Sec15, a component of the exocyst, promotes notch signaling during the asymmetric division of Drosophila sensory organ precursors. Developmental cell. 9:351–363. [PubMed: 16137928]

Kapitein LC, Schlager MA, Kuijpers M, Wulf PS, van Spronsen M, MacKintosh FC, and Hoogenraad CC. 2010. Mixed microtubules steer dynein-driven cargo transport into dendrites. Current biology : CB. 20:290–299. [PubMed: 20137950]

Kee Y, Yoo JS, Hazuka CD, Peterson KE, Hsu SC, and Scheller RH. 1997. Subunit structure of the mammalian exocyst complex. Proceedings of the National Academy of Sciences of the United States of America. 94:14438–14443. [PubMed: 9405631]

Koike S, and Jahn R. 2022. SNARE proteins: zip codes in vesicle targeting? Biochem J. 479:273–288. [PubMed: 35119456]

Koon AC, Chen ZS, Peng S, Fung JMS, Zhang X, Lembke KM, Chow HK, Frank CA, Jiang L, Lau KF, and Chan HYE. 2018. Drosophila Exo70 Is Essential for Neurite Extension and Survival under Thermal Stress. The Journal of neuroscience : the official journal of the Society for Neuroscience. 38:8071–8086. [PubMed: 30209205]

Lalli G 2009. RalA and the exocyst complex influence neuronal polarity through PAR-3 and aPKC. Journal of cell science. 122:1499–1506. [PubMed: 19383721]

Lepore DM, Martinez-Nunez L, and Munson M. 2018. Exposing the Elusive Exocyst Structure. Trends Biochem Sci. 43:714–725. [PubMed: 30055895]

Lira M, Arancibia D, Orrego PR, Montenegro-Venegas C, Cruz Y, Garcia J, Leal-Ortiz S, Godoy JA, Gundelfinger ED, Inestrosa NC, Garner CC, Zamorano P, and Torres VI. 2019. The Exocyst Component Exo70 Modulates Dendrite Arbor Formation, Synapse Density, and Spine Maturation in Primary Hippocampal Neurons. Mol Neurobiol. 56:4620–4638. [PubMed: 30374940]

Martin-Urdiroz M, Deeks MJ, Horton CG, Dawe HR, and Jourdain I. 2016. The Exocyst Complex in Health and Disease. Front Cell Dev Biol. 4:24. [PubMed: 27148529]

Mattie FJ, Stackpole MM, Stone MC, Clippard JR, Rudnick DA, Qiu Y, Tao J, Allender DL, Parmar M, and Rolls MM. 2010. Directed Microtubule Growth, +TIPs, and Kinesin-2 Are Required for Uniform Microtubule Polarity in Dendrites. Current biology : CB. 20:2169–2177. [PubMed: 21145742]

McNew JA, Parlati F, Fukuda R, Johnston RJ, Paz K, Paumet F, Sollner TH, and Rothman JE. 2000. Compartmental specificity of cellular membrane fusion encoded in SNARE proteins. Nature. 407:153–159. [PubMed: 11001046]

Murthy M, Garza D, Scheller RH, and Schwarz TL. 2003. Mutations in the exocyst component Sec5 disrupt neuronal membrane traffic, but neurotransmitter release persists. Neuron. 37:433–447. [PubMed: 12575951]

Murthy M, Ranjan R, Denef N, Higashi ME, Schupbach T, and Schwarz TL. 2005. Sec6 mutations and the Drosophila exocyst complex. Journal of cell science. 118:1139–1150. [PubMed: 15728258]

Novick P, Field C, and Schekman R. 1980. Identification of 23 complementation groups required for post-translational events in the yeast secretory pathway. Cell. 21:205–215. [PubMed: 6996832]

Nye DMR, Albertson RM, Weiner AT, Hertzler JI, Shorey M, Goberdhan DCI, Wilson C, Janes KA, and Rolls MM. 2020. The receptor tyrosine kinase Ror is required for dendrite regeneration in Drosophila neurons. PLoS biology. 18:e3000657. [PubMed: 32163406]

Pavez M, Thompson AC, Arnott HJ, Mitchell CB, D'Atri I, Don EK, Chilton JK, Scott EK, Lin JY, Young KM, Gasperini RJ, and Foa L. 2019. STIM1 Is Required for Remodeling of the Endoplasmic Reticulum and Microtubule Cytoskeleton in Steering Growth Cones. The Journal of neuroscience : the official journal of the Society for Neuroscience. 39:5095–5114. [PubMed: 31023836]

Peng Y, Lee J, Rowland K, Wen Y, Hua H, Carlson N, Lavania S, Parrish JZ, and Kim MD. 2015. Regulation of dendrite growth and maintenance by exocytosis. Journal of cell science. 128:4279–4292. [PubMed: 26483382]

Petrova V, Pearson CS, Ching J, Tribble JR, Solano AG, Yang Y, Love FM, Watt RJ, Osborne A, Reid E, Williams PA, Martin KR, Geller HM, Eva R, and Fawcett JW. 2020. Protrudin functions from the endoplasmic reticulum to support axon regeneration in the adult CNS. Nat Commun. 11:5614. [PubMed: 33154382]

Pfenninger KH 2009. Plasma membrane expansion: a neuron's Herculean task. Nature reviews. Neuroscience 10:251–261. [PubMed: 19259102]

Polgar N, and Fogelgren B. 2018. Regulation of Cell Polarity by Exocyst-Mediated Trafficking. Cold Spring Harb Perspect Biol. 10.

Rao K, Stone MC, Weiner AT, Gheres KW, Zhou C, Deitcher DL, Levitan ES, and Rolls MM. 2016. Spastin, atlastin, and ER relocalization are involved in axon but not dendrite regeneration. Molecular biology of the cell. 27:3245–3256. [PubMed: 27605706]

Rao KS, and Rolls MM. 2017. Two Drosophila model neurons can regenerate axons from the stump or from a converted dendrite, with feedback between the two sites. Neural Development. 12.

Rolls MM, Satoh D, Clyne PJ, Henner AL, Uemura T, and Doe CQ. 2007. Polarity and compartmentalization of Drosophila neurons. Neural Development. 2:7. [PubMed: 17470283]

Saeed B, Brillada C, and Trujillo M. 2019. Dissecting the plant exocyst. Curr Opin Plant Biol. 52:69–76. [PubMed: 31509792]

Schindelin J, Arganda-Carreras I, Frise E, Kaynig V, Longair M, Pietzsch T, Preibisch S, Rueden C, Saalfeld S, Schmid B, Tinevez JY, White DJ, Hartenstein V, Eliceiri K, Tomancak P, and Cardona A. 2012. Fiji: an open-source platform for biological-image analysis. Nature methods. 9:676–682. [PubMed: 22743772]

Shimono K, Fujimoto A, Tsuyama T, Yamamoto-Kochi M, Sato M, Hattori Y, Sugimura K, Usui T, Kimura K, and Uemura T. 2009. Multidendritic sensory neurons in the adult Drosophila abdomen: origins, dendritic morphology, and segment- and age-dependent programmed cell death. Neural Dev. 4:37. [PubMed: 19799768]

Stepanova T, Slemmer J, Hoogenraad CC, Lansbergen G, Dortland B, De Zeeuw CI, Grosveld F, van Cappellen G, Akhmanova A, and Galjart N. 2003. Visualization of microtubule growth in cultured neurons via the use of EB3-GFP (end-binding protein 3-green fluorescent protein). The Journal of neuroscience : the official journal of the Society for Neuroscience. 23:2655–2664. [PubMed: 12684451]

Stone MC, Albertson RM, Chen L, and Rolls MM. 2014. Dendrite injury triggers DLK-independent regeneration. Cell reports. 6:247–253. [PubMed: 24412365]

Stone MC, Nguyen MM, Tao J, Allender DL, and Rolls MM. 2010. Global up-regulation of microtubule dynamics and polarity reversal during regeneration of an axon from a dendrite. Molecular biology of the cell. 21:767–777. [PubMed: 20053676]

Stone MC, Rao K, Gheres KW, Kim S, Tao J, La Rochelle C, Folker CT, Sherwood NT, and Rolls MM. 2012. Normal Spastin Gene Dosage Is Specifically Required for Axon Regeneration. Cell reports.

Stone MC, Roegiers F, and Rolls MM. 2008. Microtubules Have Opposite Orientation in Axons and Dendrites of Drosophila Neurons. Molecular biology of the cell. 19:4122–4129. [PubMed: 18667536]

TerBush DR, Maurice T, Roth D, and Novick P. 1996. The Exocyst is a multiprotein complex required for exocytosis in Saccharomyces cerevisiae. The EMBO journal. 15:6483–6494. [PubMed: 8978675]

Thompson-Peer KL, DeVault L, Li T, Jan LY, and Jan YN. 2016. In vivo dendrite regeneration after injury is different from dendrite development. Genes & development. 30:1776–1789. [PubMed: 27542831]

Vaadia RD, Li W, Voleti V, Singhania A, Hillman EMC, and Grueber WB. 2019. Characterization of Proprioceptive System Dynamics in Behaving Drosophila Larvae Using High-Speed Volumetric Microscopy. Current biology : CB. 29:935–944 e934. [PubMed: 30853438]

Vance JE, Campenot RB, and Vance DE. 2000. The synthesis and transport of lipids for axonal growth and nerve regeneration. Biochim Biophys Acta. 1486:84–96. [PubMed: 10856715]

Vega IE, and Hsu SC. 2001. The exocyst complex associates with microtubules to mediate vesicle targeting and neurite outgrowth. The Journal of neuroscience : the official journal of the Society for Neuroscience. 21:3839–3848. [PubMed: 11356872]

Weber T, Zemelman BV, McNew JA, Westermann B, Gmachl M, Parlati F, Sollner TH, and Rothman JE. 1998. SNAREpins: minimal machinery for membrane fusion. Cell. 92:759–772. [PubMed: 9529252]

Wu B, and Guo W. 2015. The Exocyst at a Glance. Journal of cell science. 128:2957–2964. [PubMed: 26240175]

Yamanaka N, Marques G, and O'Connor MB. 2015. Vesicle-Mediated Steroid Hormone Secretion in Drosophila melanogaster. Cell. 163:907–919. [PubMed: 26544939]

Ye B, Kim JH, Yang L, McLachlan I, Younger S, Jan LY, and Jan YN. 2011. Differential regulation of dendritic and axonal development by the novel Kruppel-like factor Dar1. The Journal of neuroscience : the official journal of the Society for Neuroscience. 31:3309–3319. [PubMed: 21368042]

Ye B, Zhang Y, Song W, Younger SH, Jan LY, and Jan YN. 2007. Growing dendrites and axons differ in their reliance on the secretory pathway. Cell. 130:717–729. [PubMed: 17719548]

Highlights

- Post-developmental regrowth of axons and dendrites requires the exocyst complex.
- Axon regeneration was blocked at a step after specification of a new axon.
- Different exocyst subunits are all equally important for dendrite regeneration.

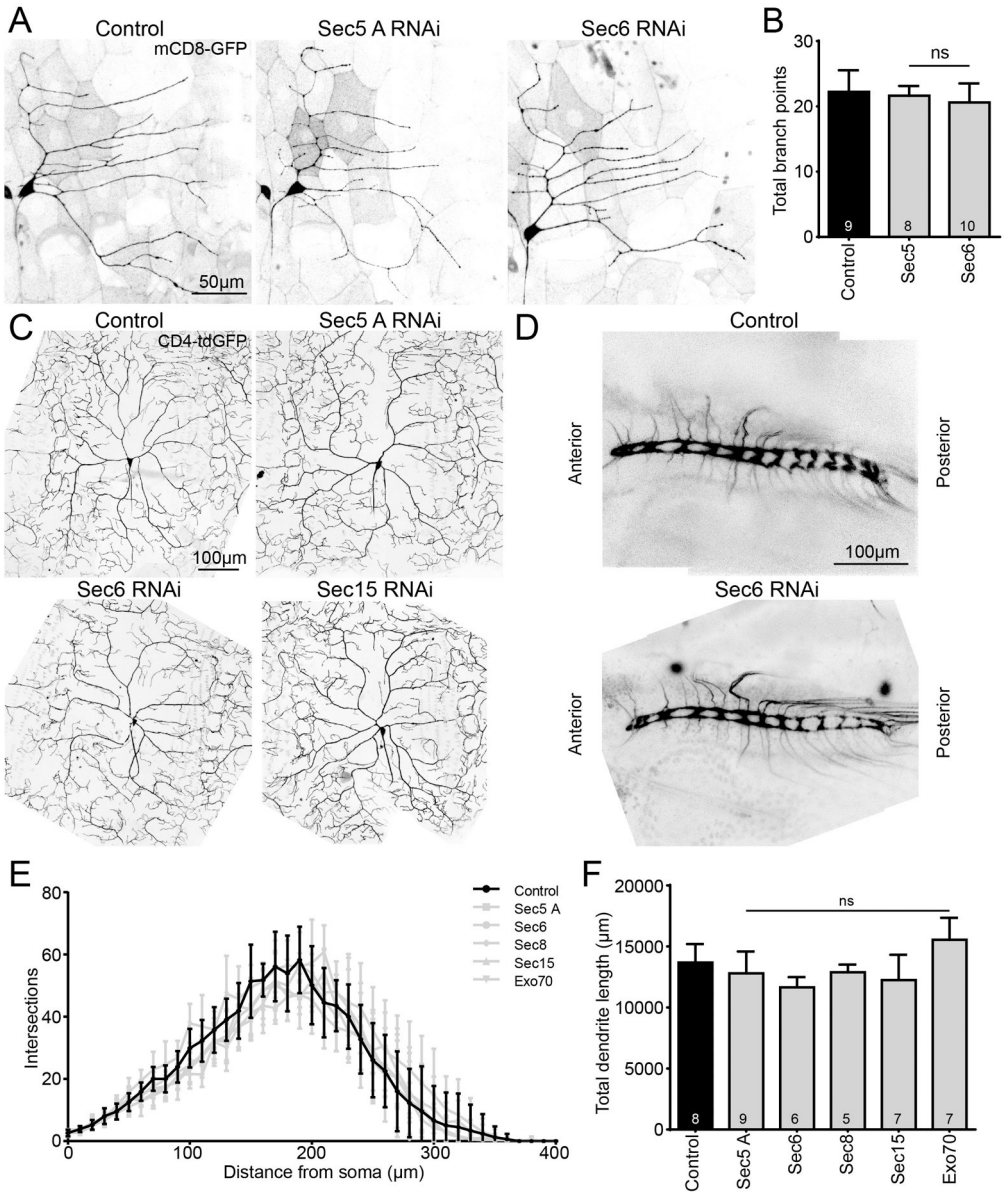

Figure 1. Exocyst RNAi does not affect initial neuronal development.

(A) Example images of class 1 ddaE neurons with control and exocyst RNAi. Average total number of dendrite branch points per neuron is quantified in (B). (C) Example images of class 4 ddaC neurons for both control and exocyst knockdown. (D) Class 4 axon terminals in the ventra nerve cord are shown. Morphology appears similar in control and neurons expressing Sec6 RNAi. (E) Sholl analysis of class 4 neurons shows no difference in dendrite complexity between control and various exocyst component knockdowns. Step size, 10μm from cell body. Each point represents the average number of intersections per step for 5-9 neurons per genotype. (F) Along with complexity, total dendrite length is unchanged (Kruskal-Wallis one-way analysis of variance with Dunn's multiple comparisons test shows no significance) by knockdown of exocyst subunits. Bars display averages of 5-9 neurons

analyzed per genotype with numbers on the bars indicating number of neurons, error bars are standard deviations.

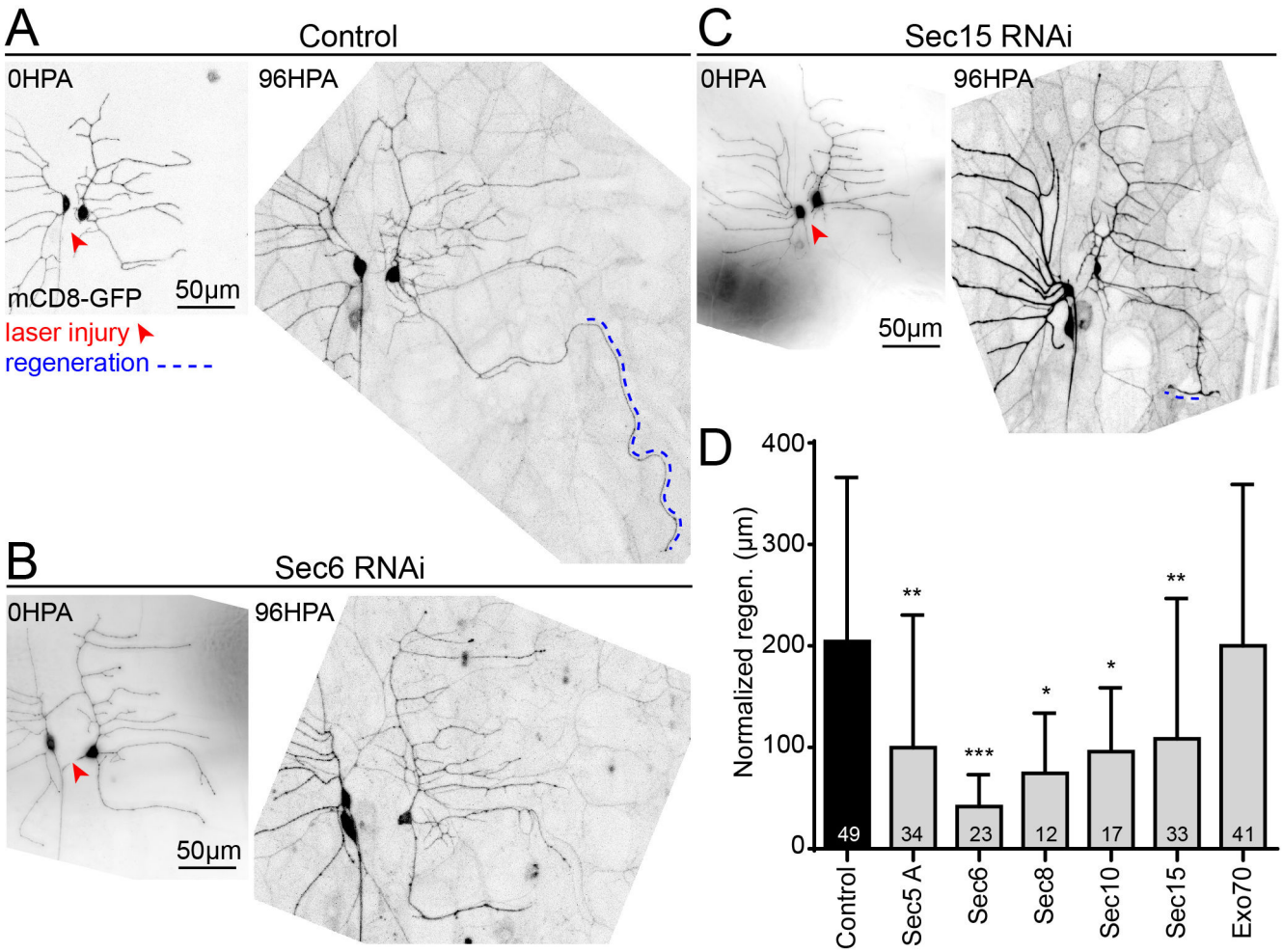

Figure 2. Exocyst knockdown strongly reduces axon regeneration.

(A) Example image of axon regeneration in neurons expressing control RNAi. A dendrite is converted to a new axon and grows outwards (blue dashed line in 96hr image). (B and C) Example images of lack of axon regeneration with Sec6 and Sec15 knockdowns are shown. (D) Quantification of normalized regeneration for all genotypes. Formula is described in methods. Bars show averages with n in each bar. Error bars are standard deviation. Sec5, Sec6, Sec8, Sec10, and Sec15 are all significantly lower than control per one-way ANOVA with Dunnett's multiple comparisons test. ***, p<.001; **, p<.01; *, p<.05.

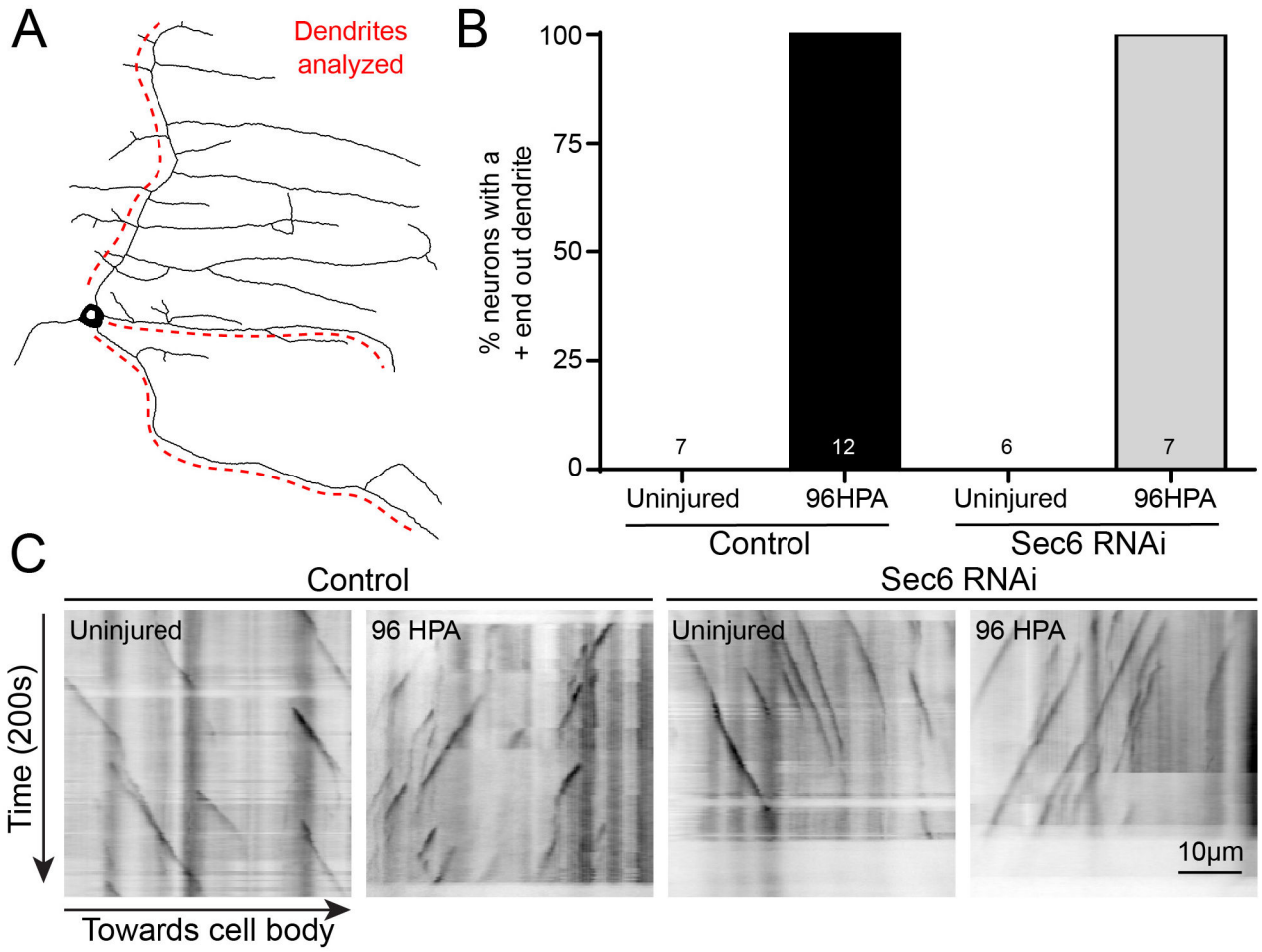

Figure 3. Exocyst RNAi neurons specify a new axon with plus-end-out microtubule polarity.

(A) Diagram of a class 1 neuron with its three main dendrites labeled. Microtubule polarity was assessed in each dendrite individually 96 hours after axotomy and in uninjured cells. (B) Class 1 neurons flip microtubule polarity from minus-end out to plus-end out in one or more dendrites to specify a new axon. The percent of injured neurons containing at least one plus-end out dendrite uninjured cells and at 96 hours post axotomy is graphed for control and Sec6 RNAi. Numbers in bars are number of neurons analyzed, with 2-3 dendrites per neuron. (C) Example kymographs showing normal minus-end out polarity in uninjured cells and plus-end out polarity 96 hours post axotomy in both genotypes.

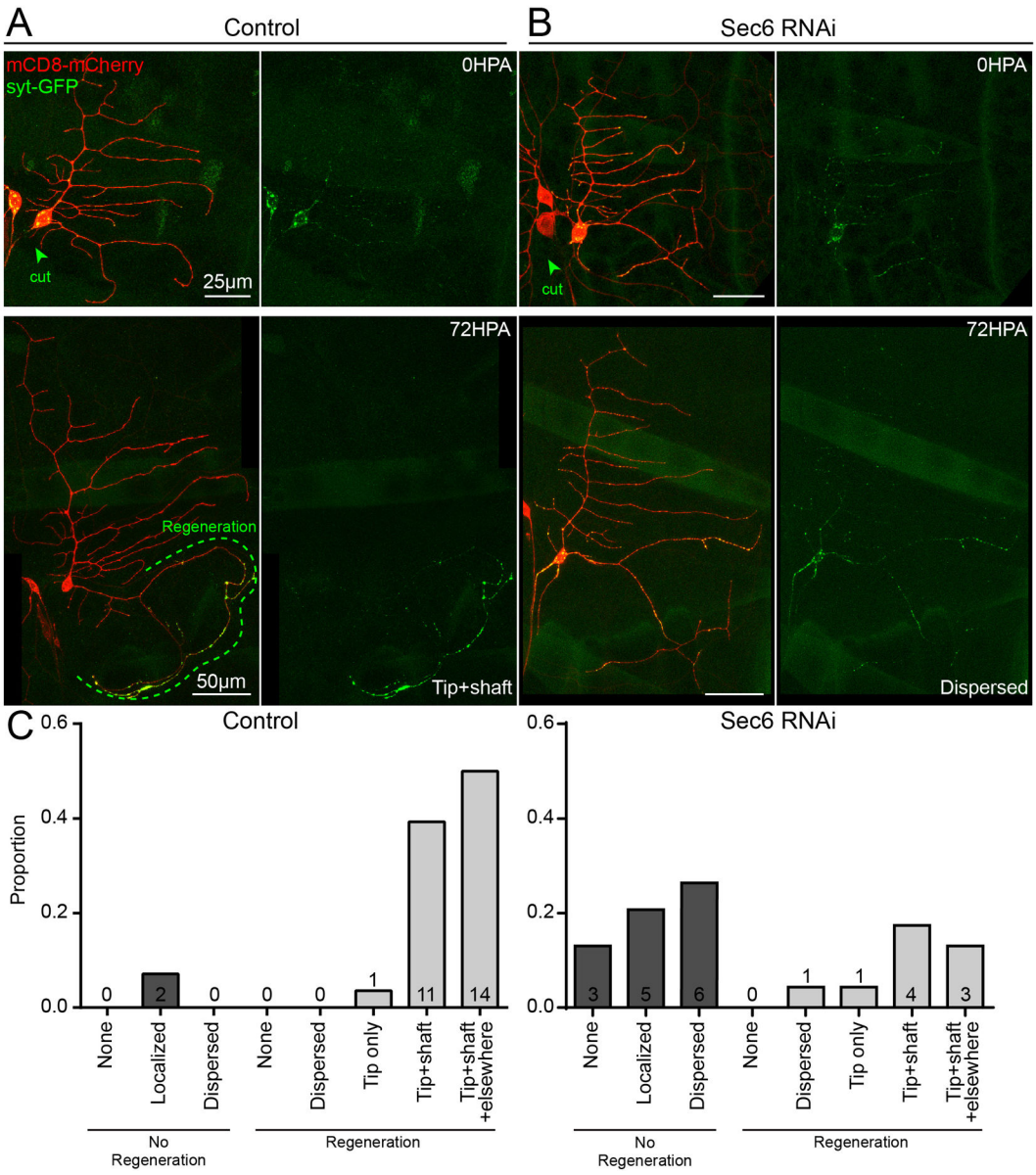

Figure 4. syt-GFP translocates to the site of axon regeneration after injury.

(A) Class I neurons expressing syt-GFP and a control RNAi were imaged before axon injury and at 72 HPA. Cut site is indicated by green arrow, and regenerating axon with dotted green line. syt-GFP appears in the regenerating tip as well as shaft of the new axon. (B) Example of neuron lacking axon regeneration with Sec6 RNAi expressed; syt-GFP can be observed in dispersed puncta throughout the dendrite arbor. (C) Quantification of different syt-GFP localization during regeneration with control and Sec6 RNAi; example images of the different categories are shown in Figure S1. Categories are described in materials and methods.

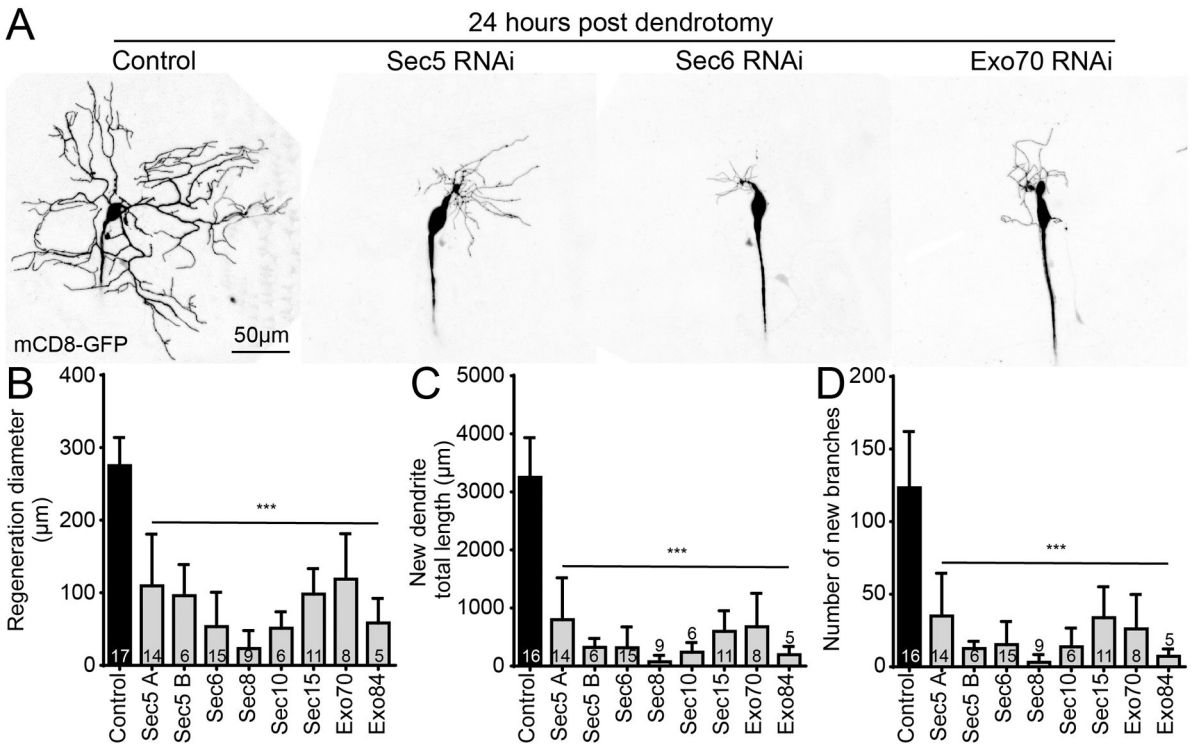

Figure 5. Exocyst knockdown causes severe deficit in dendrite regeneration.

(A) Example images of regenerating dendrites 24 hours post injury. Regeneration diameter (longest line one can draw across regenerated dendrite arbor, (B)), total new dendrite length (C), and number of new branches (D) are quantified. All genotypes are significantly different from their respective control ($p<.001$) for each of these metrics with a Kruskal-Wallis one-way ANOVA with Dunn's multiple comparisons test. Bars show averages, with number of neurons analyzed in each bar. Error bars are standard deviation. Data in (B), (C), and (D) is derived from the same images.

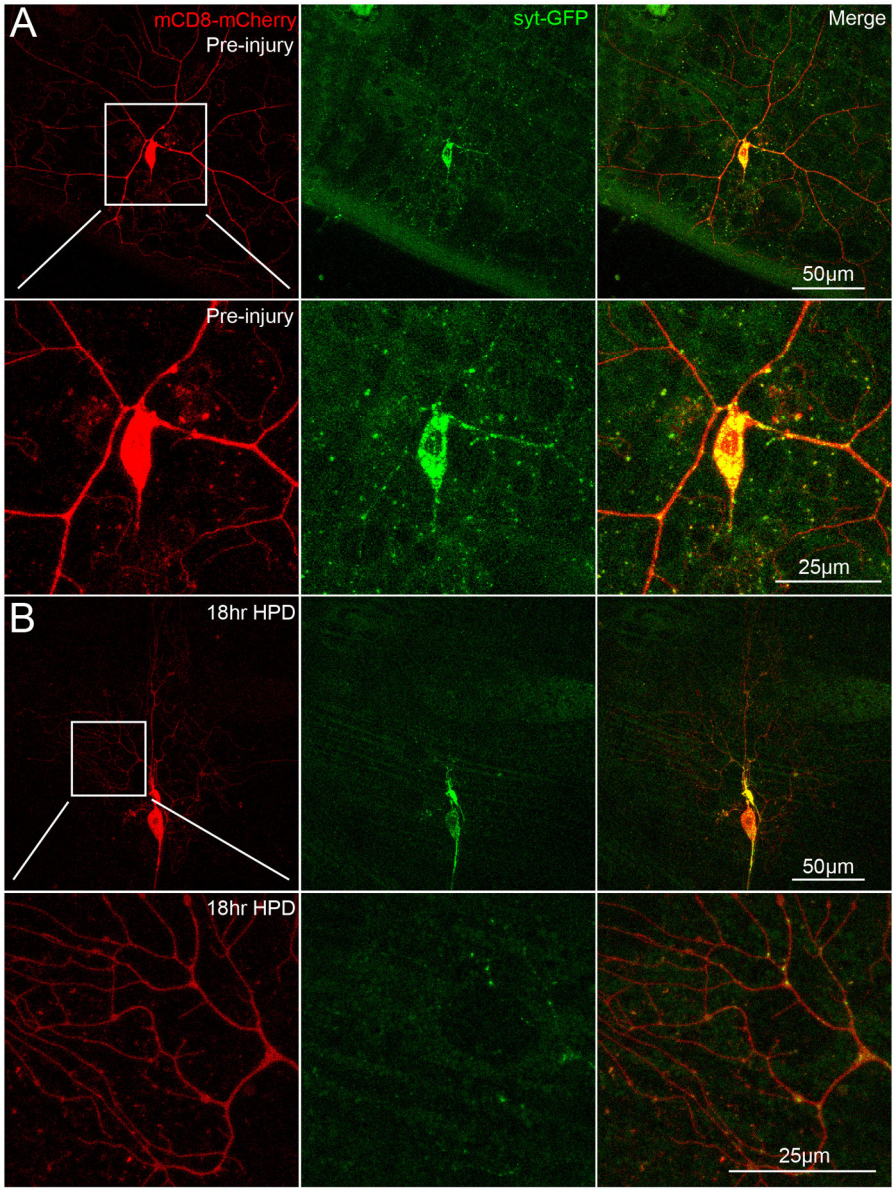

Figure 6. syt-GFP puncta populate the dendrite arbor during regeneration.

(A) In uninjured cells, syt-GFP is punctate throughout the neuron, including in axon, soma, and dendrites. (B) syt-GFP puncta can be clearly seen in the axon, soma, and regenerating dendrites. Brightness is increased for clarity.

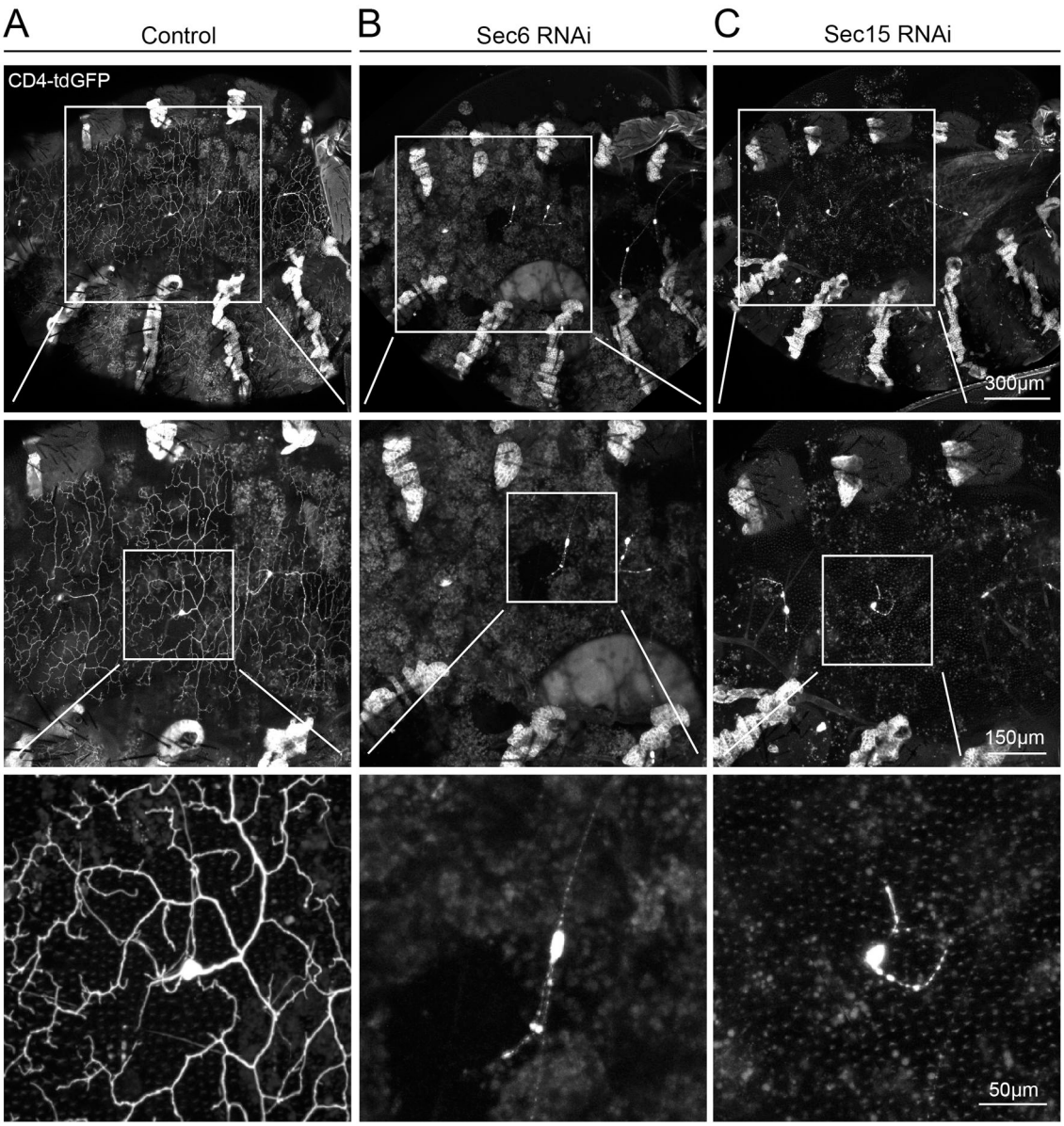

Figure 7. Dendrite regrowth during metamorphosis is abolished in exocyst knockdown neurons.

(A) Dendrites of the v'ada neurons of control flies prune to a bald cell body and subsequently regrow to innervate the adult abdomen. (B and C) When Sec6 or Sec15 are knocked down, there is no dendritic outgrowth and the cell bodies and axons appear to be degenerating. 5-6 flies were imaged for each genotype and phenotype was consistent across all animals of each genotype.

Reagent Table

A detailed description of transgenic Drosophila lines and software used in this study is provided. Transgenic lines include UAS-RNAi lines from VDRC and BDSC as well as lines with multiple transgenes that allow neuronal visualization and RNA hairpin expression.

List of RNAi lines used			
RNAi line	**Abbreviation/notes**	**Source**	**Used in paper for:**
Sec5	Sec5 A, GD RNAi collection, long hairpin	VDRC, #28873	Fig. 1,2,5
Sec5	Sec5 B, Val10 vector, long hairpin	BDSC, #27526	Fig. 5
Sec6	KK RNAi collection, long hairpin	VDRC, #105836	Fig. 1,2,3,4,5,7,S1
Sec8	Val20 vector, short hairpin	BDSC, #57441	Fig. 1,2,5
Sec10	Val10 vector, long hairpin	BDSC, #27483	Fig. 2,5
Sec15	Val10 vector, long hairpin	BDSC, #27499	Fig 1,2,5,7
Exo70	Val10 vector, long hairpin	BDSC, #28041	Fig. 1,2,5
Exo84	Val10 vector, long hairpin	BDSC, #28712	Fig. 5
gTub37c	Control	VDRC, #25271	All figs
List of lines with multiple transgenes (tester lines)			
Line		**Source**	**Used in paper for:**
UAS-Dicer-2 ; 221-Gal4, UAS-EB1-GFP		Rolls lab	Fig. 3
UAS-Dicer-2 ; 221-Gal4, UAS-mCD8-GFP		Rolls lab	Fig. 1,2
477-Gal4, UAS-mCD8-RFP		Rolls lab	Fig. 6
ppk-Gal4, ppk-EGFP, ppk-CD4-tdGFP, PXP3-nls3XTagBFP2-UAS-Dicer-2		This paper	Fig. 1,5,7
UAS-Dicer-2 ; 221-Gal4, UAS-mCD8-mCherry, UAS-synaptotagmin-GFP		This paper	Fig. 4,6,S1
Source of transgenes used in tester lines			
UAS-synaptotagmin-GFP	UAS-syt-GFP	BDSC, #6926	
UAS-Dicer-2	second chromosome	BDSC, #24650	
221-Gal4	third chromosome	Wesley Grueber	
477-Gal4	second chromosome	Wesley Grueber	
ppk-Gal4	third chromosome	Wesley Grueber	
UAS-EB1-GFP	described in Rolls, 2007	Tadashi Uemura	
ppk-EGFP	third chromosome	Wesley Grueber	
ppk-CD4-tdGFP	third chromosome	BDSC, #35843	
PXP3-nls3XTagBFP2-UAS-Dicer-2	third chromosome	This paper	
UAS-mCD8-mCherry	third chromosome	BDSC, #27392	
UAS-mCD8-RFP	second chromosome	BDSC, #27391	
Software			
Name		**Source**	**Used in paper for:**
FIJI - ImageJ		NIH: https://fiji.sc/	All figures
GraphPad Prism 7		https://www.graphpad.com/scientific-software/prism/	Fig. 1,2,3,4,5